Journal of Hazardous Materials 173 (2010) 539–543

Contents lists available at ScienceDirect

Journal of Hazardous Materials

journal homepage: www.elsevier.com/locate/jhazmat

Synergistic effects of hollow structure and surface fluorination on the photocatalytic activity of titania

Kangle Lv[a,b,*], Jiaguo Yu[b,**], Kejian Deng[a], Jie Sun[a], Yanxi Zhao[a], Dongyun Du[a], Mei Li[a]

[a] Key Laboratory of Catalysis and Materials Science of the State Ethnic Affairs Commission & Ministry of Education, South-Central University for Nationalities, Wuhan 430074, China
[b] State Key Laboratory of Advanced Technology for Materials Synthesis and Processing, Wuhan University of Technology, Wuhan 430070, China

ARTICLE INFO

Article history:
Received 29 June 2009
Received in revised form 21 August 2009
Accepted 25 August 2009
Available online 31 August 2009

Keywords:
Titania
Hollow microsphere
Nanoparticles
Surface fluorination
Photocatalytic degradation

ABSTRACT

To study the synergistic effects of hollow structure and surface fluorination on the photoactivity of TiO_2, TiO_2 hollow microspheres were synthesized by a hydrolysis–precipitate method using sulfonated polystyrene (PS) as templates and tetrabutylorthotitanate (TBOT) as precursor, and then calcined at 500 °C for 2 h. The calcined samples were characterized by X-ray diffraction, scanning electron microscopy, transmission electron microscopy and N_2 sorption. Photocatalytic activity was evaluated using reactive brilliant red X3B, an anionic organic dye, as a model pollutant in water. The results show that the photocatalytic activity of TiO_2 hollow microspheres is significantly higher than that of TiO_2 nanoparticles prepared in the same experimental conditions. At pH 7 and 3, the apparent rate constants of the former exceed that of the latter by a factor of 3.38 and 3.15, respectively. After surface fluorination at pH 3, the photoactivity of hollow microspheres and nanoparticles further increases for another 1.61 and 2.19 times, respectively. The synergistic effect of surface fluorination and hollow structure can also be used to prepare other highly efficient photocatalyst.

1. Introduction

A great deal effect has been devoted in recent decades in solving the widespread problem of contamination of effluent from urban and agricultural industries with biorecalcitrant and organic pollutants [1–9]. Various catalytic techniques have been applied in the field of environmental protection. Among which, TiO_2 photocatalysis has attracted increasing attention due to its biological and chemical inertness, strong photo oxidization power, cost effectiveness, and long-term stability against photo and chemical corrosion [8–12]. However, a vital problem, i.e., low quantum efficiency (~4%), hampers its widespread practical applications [10,13,14]. To improve these properties, the morphologies and macroscopic structures of TiO_2 have been intensively studied [13,15–17]. For example, a three-dimensional porous structure of TiO_2 with a large surface area is known to exhibit an enhanced photocatalytic performance [18,19]. The submicron-scale hollow spheres of TiO_2 are promising because of their potential to provide a large surface/volume ratio [17,19]. In addition, the diffractions on the hollow spheres and the reflections due to the shell structure would improve the functional properties of TiO_2 [13,19]. It has been recently reported that surface fluorination can result in significant enhancement in the photocatalytic activity of TiO_2, ascribed to the enhanced production of free •OH radicals in solution as a result of fluoride displacement of surface hydroxyl groups (Eqs. (1) and (2)) [11,12,20,21]. Interestingly, Choi and co-workers have demonstrated that the surface fluorination of TiO_2 also result in the enhanced photocatalytic degradation of stearic acid [22] and acetaldehyde [23] in gaseous phase, and they ascribed this to the enhanced generation of airborne free •OH radicals.

$$\equiv Ti\text{–}OH + F^- \rightarrow \equiv Ti\text{–}F + OH^- \quad (1)$$

$$\equiv Ti\text{–}F + H_2O + h_{vb}{}^+ \rightarrow \equiv Ti\text{–}F + {}^{\bullet}OH_{free} + H^+ \quad (2)$$

However, the synergistic effects of hollow structure and surface fluorination on the photoactivity of TiO_2 have not been reported yet. In the present work, we prepared hollow spheres of TiO_2 using sulfonated polystyrene (PS) as template, and the effect of surface fluorination on the photoactivity of hollow microspheric TiO_2 is examined, using reactive brilliant red X3B [10], an anionic organic dye, as the target organic pollutant.

* Corresponding author at: State Key Laboratory of Advanced Technology for Materials Synthesis and Processing, Wuhan University of Technology, Luoshi Road 122#, Wuhan 430070, China. Tel.: +86 27 87952410; fax: +86 27 87952410.
** Corresponding author. Tel.: +86 27 87871029; fax: +86 27 87879468.
E-mail addresses: lvkangle@mail.scuec.edu.cn (K. Lv), jiaguoyu@yahoo.com (J. Yu).

0304-3894/$ – see front matter © 2009 Elsevier B.V. All rights reserved.
doi:10.1016/j.jhazmat.2009.08.119

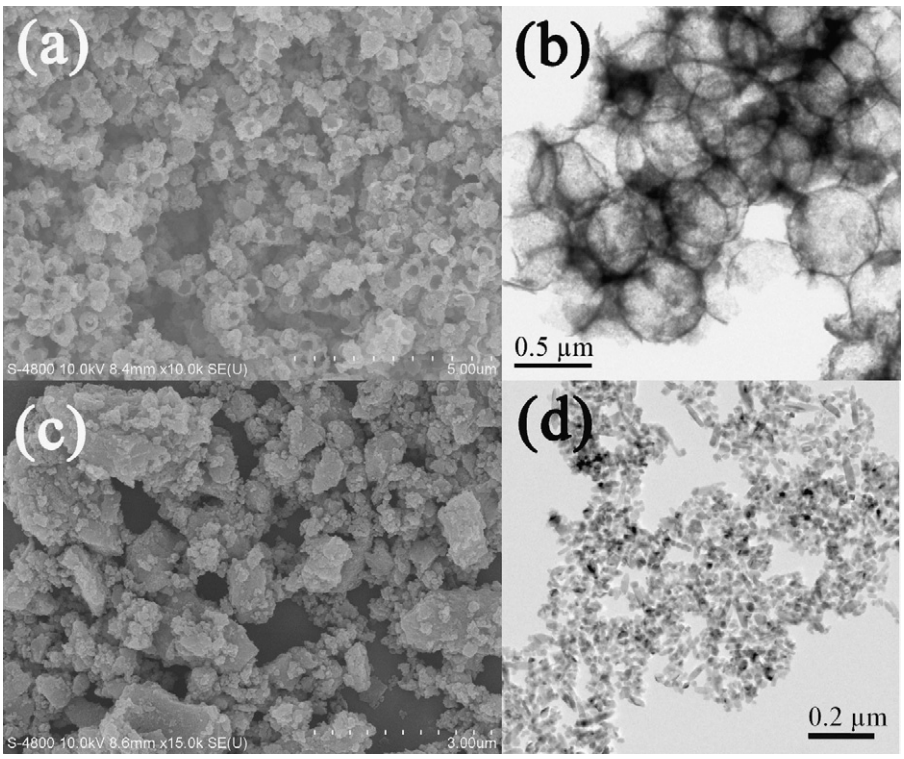

Fig. 1. SEM and TEM images of TiO_2 hollow microspheres (A and B) and nanoparticles (C and D).

2. Experimental

2.1. Preparation

Template of sulfonated PS with a diameter of 0.5 μm is prepared according to the literature [24], then 25 mL ethanol solution containing 0.3 mL tetrabutylorthotitanate (TBOT) was added dropwise to 15 mL of the sulfonated PS spheres ethanol solution (0.1 g/mL) under magnetic stirring. After that, 25 mL of ethanol solution containing 3.4 mL ammonia solution was dropped into the mixed solution. The resulted solution was stirred at 60 °C for another 2 h before it was refluxed for another 1.5 h. The solution was then filtered and the cake was washed with ethanol and water. TiO_2 hollow spheres were obtained after the cake was heated in air at 500 °C for 2 h to remove the PS templates. TiO_2 nanoparticles were also prepared accordingly in the absence of sulfonated PS template.

2.2. Characterization

The X-ray diffraction (XRD) patterns obtained on a D8 advance X-ray diffractometer (German Bruker) using Cu Kα radiation at a scan rate of 0.02°/s were used to determine the crystallite size and identity. The accelerated voltage and applied current were 200 kV and 20 mA, respectively. The average crystallite size of the catalyst was determined according to the Scherrer equation using FWHM data after correcting for the instrumental broadening. The BET surface area (S_{BET}) of the powders was analyzed using nitrogen adsorption in a Micromeritics ASAP 2020 nitrogen-adsorption apparatus (USA). The BET surface area was determined by a multipoint BET method using the adsorption data in the relative pressure (P/P_0) range of 0.05–0.3. Pore volume and average pore size (APS) were determined by nitrogen-adsorption volume at the relative pressure of 0.994. All the samples were degassed at 180 °C prior to the nitrogen-adsorption measurements. The morphologies of TiO_2 powders were observed on a field emission scanning electron microscope (SEM) (Hitach, Japan) with an acceleration voltage of 20 kV and transmission electron microscope (TEM) (Tecnai G20, USA) using an acceleration voltage of 200 kV.

2.3. Adsorption and photoactivity evaluation

Photocatalytic reactions were carried out using a high-pressure mercury lamp (375 W, Shanghai Yamin) as light source, emitted mainly at 365 nm. The reactor (80 mL) was made of a Pyrex glass, and positioned at a fixed distance of ca. 10 cm from the lamp. X3B was used as the target organic pollutant. $HClO_4$ and NaOH were used to adjust the solution pH, and NaF (1.0 mM), if necessary, was added in the solution for surface fluorination of TiO_2. Prior to illumination, a suspension containing 50.0 mg of catalyst and 50 mL of 1.0×10^{-4} mol/L X3B was continuously stirred in the dark for 12 h. The concentration of substrate in bulk solution at this point was used as the initial value for the adsorption and the further kinetic treatment of the photodegradation processes. During the photoreaction, the reactor was thermostated at 25 °C through a water recycle system and stirred mechanically at a constant rate. At given intervals of illumination, small aliquots of the suspension were withdrawn by syringe, centrifuged, and then filtered through a Millipore filter (pore size 0.45 μm). The filtrates were monitored by a UV–vis spectroscopy at 510 nm.

3. Results and discussion

3.1. Morphology and crystalline phase

Fig. 1A and B shows SEM and TEM images of the titania hollow microspheres prepared in the presence of spheric sulfonated PS template, respectively. In this preparation approach, TBOT is firstly adsorbed into the negatively charged sulfonated shell layer of PS templates [13]. After hydrolysis in a basic solution and calcinations, the PS template is removed and the hollow spheres of TiO_2 are obtained. The prepared TiO_2 hollow microspheres are monodispersed in a diameter of 0.5 μm and a shell thickness of 10–20 nm

Table 1
Physical properties of the photocatalysts.

Photocatalyst	Phase	Crystalline size (nm)	S_{BET} (m^2/g)	Pore volume (cm^3/g)	APS (nm)
Nanoparticles	Anatase	26.2	14.0	0.071	9.8
Hollow spheres	Anatase	13.5	32.9	0.12	14.2

(Fig. 1A and B). However, only TiO_2 aggregated nanoparticles are accordingly obtained in the absence of sulfonated PS template (Fig. 1C and D).

XRD results (not shown here) indicate that the diffraction peaks of the TiO_2 hollow spheres and nanoparticles could be indexed as the tetragonal anatase TiO_2, which are in good agreement with the JCPDS file of TiO_2 (JCPDS No. 21-1272) [16]. According to the Scherrer–Warren formula, the average crystallite size of the TiO_2 hollow spheres and nanoparticles after calcination are around 13.5 and 26.2 nm, respectively (Table 1). The smaller crystallite size of the TiO_2 hollow spheres is due to the low hydrolysis reaction rate of TBOT adsorbed on the surface of sulfonated PS and these adsorbed sulfonated groups prevent the crystallization of the TiO_2 hollow spheres.

3.2. BET surface areas and pore structures

The N_2 adsorption–desorption isotherms of the TiO_2 hollow microspheres and nanoparticles are of type IV (Fig. 2). At low relative pressure, the adsorption isotherm of TiO_2 hollow microspheres is higher than that of TiO_2 nanoparticles. It demonstrates that TiO_2 hollow microspheres contain more micropores than nanoparticles due to its smaller crystallite size of 13.5 nm (Table 1). At high relative pressure between 0.4 and 1.0, the curve exhibits a hysteresis loop, implying the presence of mesopores (type IV) [6,14]. The hysteresis loop of TiO_2 nanoparticles at high relative pressure is more obvious than that of hollow microspheres, indicating a narrower mesopore size distribution of TiO_2 nanoparticles (Fig. 2). The micropores and small mesopores in TiO_2 hollow spheres are from intra-aggregated pores, and the large mesopores may be assigned to the pores among inter-aggregated particles [25,26]. In comparison with nanoparticles, TiO_2 hollow microspheres show a larger specific surface area, pore volume and smaller average pore size (APS) with the values of 32.9 m^2/g, 0.12 cm^3/g and 14.2 nm, respectively. The corresponding values for that of nanoparticles are 14.0 m^2/g, 0.071 cm^3/g and 9.8 nm, respectively (Table 1).

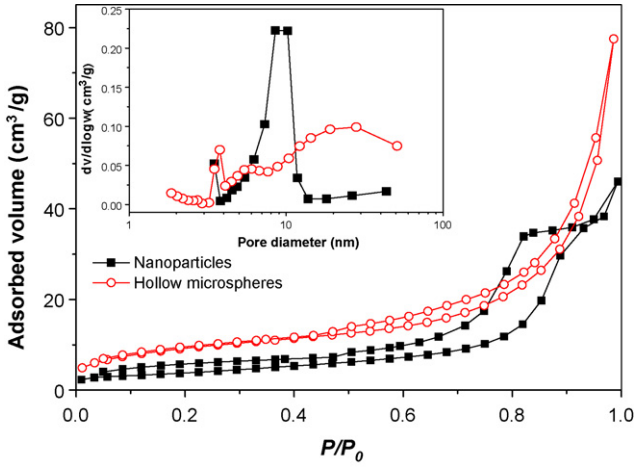

Fig. 2. N_2 adsorption–desorption isotherms and corresponding pore size distributions (inset) of the prepared titania nanoparticles and hollow microspheres.

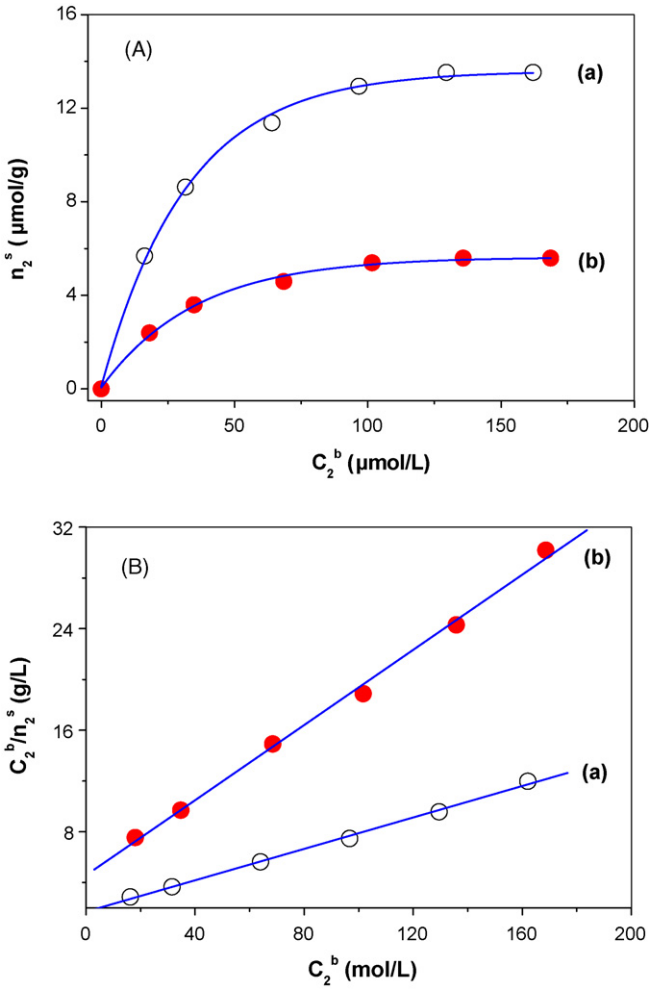

Fig. 3. Adsorption isotherm (A) and the corresponding Langmuir plot (B) of X3B on TiO_2 samples of hollow microspheres (a) and nanoparticles (b), from aqueous solution (pH 7) at 25 °C.

3.3. Adsorption of X3B at pH 7

Dark adsorption properties of the catalyst are important to the surface photoreaction and the determination of reaction rate as well [27]. The adsorption capacity of the catalyst for the organic substrate of X3B in water was thus measured at pH 7. Fig. 3A demonstrates the adsorption isotherms of the prepared TiO_2, where the amount of equilibrium adsorption, n_2^s, is plotted as a function of equilibrium concentration in bulk solution, C_2^b. It can be seen that the adsorption of TiO_2 hollow microspheres were much higher than that of nanoparticles, in agreement with the order of S_{BET}. Larger surface area is expected to have more sites for X3B to be adsorbed. The adsorption of X3B on TiO_2 can be described by the Langmuir model with an equation of $n_2^s = n^s K C_2^b/(1 + K C_2^b)$ [10,27], where n^s is the total adsorption sites and K is the Langmuir adsorption constant. The adsorption parameters of n^s and K can easily be obtained from Fig. 3B. It can be seen from Table 2 that TiO_2 hollow microspheres exhibit larger adsorption parameters of n^s and K than nanoparticles. This difference can be attributed to the TiO_2 hol-

Table 2
Adsorption and photoactivity of the photocatalysts.

Photocatalyst	n^s (μmol/g)[a]	K (L/mol)[a]	n_{ad} (μmol/g)[b]			K_{app} (10^{-3} min^{-1})		
			pH 7	pH 3	pH 3/F	pH 7	pH 3	pH 3/F
Nanoparticles	6.80	3.24×10^4	5.38	31.9	6.30	7.87	6.68	14.63
Hollow spheres	16.2	3.64×10^4	12.9	49.8	12.4	26.59	21.02	33.80

[a] The maximum adsorbed amount and the adsorption constant of X3B on the surface of TiO_2 at pH 7, according to Langmuir model with an equation of $n_2^s = n^s KC_2^b/(1 + KC_2^b)$.
[b] The amount of X3B adsorbed on the surface of TiO_2 after adsorption–desorption equilibrium is reached (initial concentration of X3B is 1.0×10^{-4} mol/L).

low microspheres with smaller crystallite size and higher specific surface areas. As reported by Xu and Langford [27] the adsorption constant K increases with decreasing the particle size because of a greater driving force for adsorption on the finer particles.

3.4. Photocatalytic degradation

X3B is a very stable organic chemical and it shows little degradation under UV irradiation ($\lambda \geq 320$ nm) in the absence of photocatalyst [10,13]. The degradation kinetics of X3B in the presence of TiO_2 can be well fitted by the apparent first-order rate equation. TiO_2 hollow microspheres show much higher photoactivity than that of nanoparticles at pH 7 (Fig. 4c and b). The apparent rate constant (K_{app}) of the former exceeds that of the latter by a factor of 3.38 (26.59×10^{-3} min^{-1} for hollow microspheres and 7.87×10^{-3} min^{-1} for nanoparticles), which are ascribed to the stronger adsorptive ability of hollow microspheres due to their smaller particle size and larger surface areas (Table 1). As a naked TiO_2 particle is exposed to water, the surface is hydrated to satisfy the coordination of surface Ti^{VI} ions. Dissociation of the chemisorbed molecular water then gives rise to surface OH^- groups (≡Ti–OH), consequently, the surface of TiO_2 becomes positively charged in an acidic medium. The surface specification modeling shows that ≡Ti–OH_2^+ species accounts for 89% at pH 3 [20]. Thus, a high adsorption of anionic X3B on TiO_2 was observed at pH 3. The adsorption of fluoride on TiO_2 is a ligand exchange between F^- and ≡Ti–OH on the surface (Eq. (1)). Such complexation is more favorable in an acidic medium (especially at pH 3), with an equilibrium constant of about 10^8 [10,20,21]. The surface specification modeling shows that ≡Ti–F is the dominant species on the surface of TiO_2 in the presence of 1.0 mM NaF at pH 3 [10]. The positive charge of TiO_2 (≡Ti–OH_2^+) is reduced after the surface is occupied by fluoride, which leads to a decrease in the adsorption of X3B (Table 2).

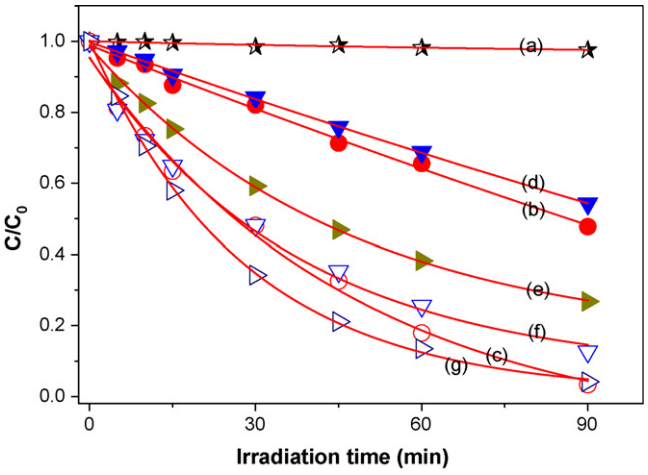

Fig. 4. Photocatalytic degradation of X3B under UV irradiation at different experimental conditions, (a) in the solution of 1.0 mM NaF at pH 3 without photocatalyst, (b) in the presence of titania nanoparticles at pH 7, (c) in the presence of hollow microspheres at pH 7, (d) in the presence of naked titania nanoparticles at pH 3, (e) in the presence of fluorinated titania nanoparticles at pH 3, (f) in the presence of naked titania hollow microspheres at pH 3 and (g) in the presence of fluorinated titania hollow microspheres at pH 3.

To study the synergistic effect of surface fluorination and hollow microstructure on the photoactivity of TiO_2, photocatalytic degradation of X3B was performed at pH 3. It should be noted that the degradation of X3B under UV is negligible in a homogeneous NaF solution at pH 3 without the photocatalyst (Fig. 4a). Although the adsorption isotherms of X3B at pH 3, in TiO_2 hollow microspheres and nanoparticles, are not determined, the amount of X3B adsorbed (n_{ad}) before irradiation at the same initial concentration could also be served as a qualitative reference for the comparison in adsorption. Table 2 shows the amount of X3B adsorbed on the surface of TiO_2 after adsorption–desorption equilibrium is reached at pH 7 and pH 3 in the presence or absence of NaF (initial concentration of X3B is 1.0×10^{-4} mol/L). It suggests that the adsorption of X3B on the surface of TiO_2 hollow microspheres is much higher than on the surface of nanoparticles at pH 3. The degradation profiles of X3B at pH 3 in TiO_2 hollow microspheres and nanoparticles are shown in Fig. 4f and d, respectively. The apparent rate constant of the former exceeds that of the latter by a factor of 3.15 (21.02×10^{-3} min^{-1} for hollow microspheres and 6.68×10^{-3} min^{-1} for nanoparticles). After surface fluorination, the degradation of X3B is greatly enhanced, in solutions of TiO_2 nanoparticles and hollow microspheres (Fig. 4e and g). The photoactivity of hollow microspheres and nanoparticles further increases for another 1.61 and 2.19 times (14.63×10^{-3} min^{-1} for hollow microspheres and 33.80×10^{-3} min^{-1} for nanoparticles), respectively.

It is assumed that the relative reactivity of free hydroxyl radicals is higher than that of subsurface holes [10]. The enhanced photoactivity of TiO_2 after surface fluorination is due to the transformation of active species from hole to free hydroxyl radical (Eq. (1) and (2)). Fig. 4 shows that TiO_2 hollow microspheres after surface fluorination exhibits the highest photoactivity in all situations, which reflects the synergistic effects of hollow structure and surface fluorination on the photoactivity of TiO_2. Some papers reported that the high photoreactivity of the TiO_2 hollow spheres is due to the multiple diffractions and reflections of the light irradiated on the surface of the catalyst [15,19,28,29]. However, in our case, TiO_2 hollow spheres show the same light absorptive ability as that of nanoparticles according to the diffused reflectance spectra (data not shown here), which suggested that it should be other factors, such as adsorption, other than light harvesting ability of the photocatalysts, to be responsible for the higher photoactivity of hollow spheres.

4. Conclusions

The effect of surface fluorination and hollow structure on the photoactivity of TiO_2 is studied. It demonstrates that the adsorption and photoactivity of TiO_2 hollow microspheres are higher than that of nanoparticles due to its stronger adsorption to the substrate, owing to the smaller particle size and larger surface area. Surface fluorination can further enhance the photoactivity, and the TiO_2 hollow microspheres after fluorination shows the highest photoactivity, which demonstrates the synergistic effect of sur-

face fluorination and hollow structure on the photoactivity of TiO_2. This study may provide new insight into design and preparation of advanced photocatalytic materials.

Acknowledgements

This work was partially supported by the National Natural Science Foundation of China (50625208, 20773097 and 20877061), Natural Science Foundation of Hubei Province (2008CDB265) and China Postdoctoral Science Foundation (20090451086). This work was also financially supported by the National Basic Research Program of China (2007CB613302).

References

[1] T. Giannakopoulou, N. Todorova, C. Trapalis, T. Vaimakis, Effect of fluorine doping and SiO_2 under-layer on the optical properties of TiO_2 thin films, Mater. Lett. 61 (2007) 4474–4477.
[2] H.C. Liang, X.Z. Li, Effects of structure of anodic TiO_2 nanotube arrays on photocatalytic activity for the degradation of 2,3-dichlorophenol in aqueous solution, J. Hazard. Mater. 162 (2009) 1415–1422.
[3] Y.X. Li, G.F. Ma, S.Q. Peng, G.X. Lu, S.B. Li, Boron and nitrogen co-doped titania with enhanced visible-light photocatalytic activity for hydrogen evolution, Appl. Surf. Sci. 254 (2008) 6831–6836.
[4] Z.L. Jin, X.J. Zhang, Y.X. Li, S.B. Li, G.X. Lu, 5.1% apparent quantum efficiency for stable hydrogen generation over eosin-sensitized CuO/TiO_2 photocatalyst under visible light irradiation, Catal. Commun. 8 (2007) 1267–1273.
[5] F.B. Li, X.Z. Li, C.H. Ao, S.C. Lee, M.F. Hou, Enhanced photocatalytic degradation of VOCs using Ln^{3+}–TiO_2 catalysts for indoor air purification, Chemosphere 59 (2005) 787–800.
[6] V. Balek, N. Todorova, C. Trapalis, V. Stengl, E. Vecernikova, J. Subrt, Z. Malek, G. Kordas, Thermal behavior of Fe_2O_3/TiO_2 mesoporous gels, J. Therm. Anal. Calorim. 80 (2005) 503–509.
[7] J.G. Yu, L.J. Zhang, B. Cheng, Y.R. Su, Hydrothermal preparation and photocatalytic activity of hierarchically sponge-like macro-/mesoporous titania, J. Phys. Chem. C 111 (2007) 10582–10589.
[8] J.G. Yu, S.W. Liu, H.G. Yu, Microstructures and photoactivity of mesoporous anatase hollow microspheres fabricated by fluoride-mediated self-transformation, J. Catal. 249 (2007) 59–66.
[9] J.G. Yu, S.W. Liu, M.H. Zhou, Enhanced photocalytic activity of hollow anatase microspheres by Sn^{4+} incorporation, J. Phys. Chem. C 112 (2008) 2050–2057.
[10] K.L. Lv, Y.M. Xu, Effects of polyoxometalate and fluoride on adsorption and photocatalytic degradation of organic dye X3B on TiO_2: the difference in the production of reactive species, J. Phys. Chem. B 110 (2006) 6204–6212.
[11] Y.M. Xu, K.L. Lv, Z.G. Xiong, W.H. Leng, W.P. Du, D. Liu, X.J. Xue, Rate enhancement and rate inhibition of phenol degradation over irradiated anatase and rutile TiO_2 on the addition of NaF: new insight into the mechanism, J. Phys. Chem. C 111 (2007) 19024–19032.
[12] J.G. Yu, W.G. Wang, B. Cheng, B.L. Su, Enhancement of photocatalytic activity of mesporous TiO_2 powders by hydrothermal surface fluorination treatment, J. Phys. Chem. C 113 (2009) 6743–6750.
[13] X.F. Li, K.L. Lv, K.J. Deng, J.F. Tang, R. Su, J. Sun, L.Q. Chen, Synthesis and characterization of ZnO and TiO_2 hollow spheres with enhanced photoreactivity, Mater. Sci. Eng. B 158 (2009) 40–47.
[14] M.H. Zhou, J.G. Yu, B. Cheng, Effects of Fe-doping on the photocatalytic activity of mesoporous TiO_2 powders prepared by an ultrasonic method, J. Hazard. Mater. 137 (2006) 1838–1847.
[15] Y. Kondo, H. Yoshikawa, K. Awaga, M. Murayama, T. Mori, K. Sunada, S. Bandow, S. Iijima, Preparation, photocatalytic activities, and dye-sensitized solar-cell performance of submicron-scale TiO_2 hollow spheres, Langmuir 24 (2008) 547–550.
[16] J.G. Yu, W. Liu, H.G. Yu, A one-pot approach to hierarchically nanoporous titania hollow microspheres with high photocatalytic activity, Cryst. Growth Des. 8 (2008) 930–934.
[17] J.H. Pan, X.W. Zhang, A.J. Du, D.D. Sun, J.O. Leckie, Self-etching reconstruction of hierarchically mesoporous F–TiO_2 hollow microspherical photocatalyst for concurrent membrane water purifications, J. Am. Chem. Soc. 130 (2008) 11256–11257.
[18] Y.Z. Li, T. Kunitake, S. Fujikawa, Efficient fabrication and enhanced photocatalytic activities of 3D-ordered films of titania hollow spheres, J. Phys. Chem. B 110 (2006) 13000–13004.
[19] H.X. Li, Z.F. Bian, J. Zhu, D.Q. Zhang, G.S. Li, Y.N. Huo, H. Li, Y.F. Lu, Mesoporous titania spheres with tunable chamber structure and enhanced photocatalytic activity, J. Am. Chem. Soc. 129 (2007) 8406–8407.
[20] C. Minero, G. Mariella, V. Maurino, E. Pelizzetti, Photocatalytic transformation of organic compounds in the presence of inorganic anions. 1. Hydroxyl-mediated and direct electron-transfer reactions of phenol on a titanium dioxide–fluoride system, Langmuir 16 (2000) 2632–2641.
[21] K.L. Lv, C.S. Lu, Different effects of fluoride surface modification on the photocatalytic oxidation of phenol in anatase and rutile TiO_2 suspensions, Chem. Eng. Technol. 31 (2008) 1272–1276.
[22] J.S. Park, W.Y. Choi, Enhanced remote photocatalytic oxidation on surface-fluorinated TiO_2, Langmuir 20 (2004) 11523–11527.
[23] H.J. Kim, W.Y. Choi, Effects of surface fluorination of TiO_2 on photocatalytic oxidation of gaseous acetaldehyde, Appl. Catal. B 69 (2007) 127–132.
[24] Z.W. Deng, M. Chen, G.X. Gu, L.M. Wu, A facile method to fabricate ZnO hollow spheres and their photocatalytic property, J. Phys. Chem. B 112 (2008) 16–22.
[25] J.G. Yu, M.H. Zhou, B. Cheng, H.G. Yu, X.J. Zhao, Ultrasonic preparation of mesoporous titanium dioxide nanocrystalline photocatalysts and evaluation of photocatalytic activity, J. Mol. Catal. A 227 (2005) 75–80.
[26] J.G. Yu, M.H. Zhou, B. Cheng, X.J. Zhao, Preparation, characterization and photocatalytic activity of in situ N,S-codoped TiO_2 powders, J. Mol. Catal. A 246 (2006) 176–184.
[27] Y.M. Xu, C.H. Langford, UV- or visible-light-induced degradation of X3B on TiO_2 nanoparticles: the influence of adsorption, Langmuir 17 (2001) 897–902.
[28] J.G. Yu, L.F. Qi, B. Cheng, X.F. Zhao, Effect of calcination temperatures on microstructures and photocatalytic activity of tungsten trioxide hollow microspheres, J. Hazard. Mater. 160 (2008) 621–628.
[29] J.G. Yu, L.F. Qi, Template-free fabrication of hierarchically flower-like tungsten trioxide assemblies with enhanced visible-light-driven photocatalytic activity, J. Hazard. Mater. 169 (2009) 221–227.